Enhanced gross primary production and evapotranspiration in juniper-encroached grasslands

Jie Wang[1], Xiangming Xiao[1,2], Yao Zhang[1,3], Yuanwei Qin[1], Russell B. Doughty[1], Xiaocui Wu[1], Rajen Bajgain[1], Ling Du[1]

[1] Department of Microbiology and Plant Biology, Center for Spatial Analysis, University of Oklahoma, Norman, Oklahoma [2] Ministry of Education Key Laboratory of Biodiversity Science and Ecological Engineering, Institute of Biodiversity Science, Fudan University, Shanghai, China [3] Department of Earth and Environment Engineering, Columbia University, New York, New York

Correspondence Xiangming Xiao, Department of Microbiology and Plant Biology, University of Oklahoma, Norman, OK. Email: xiangming.xiao@ou.edu

Abstract

Woody plant encroachment (WPE) into grasslands has been occurring globally and may be accelerated by climate change in the future. This land cover change is expected to alter the carbon and water cycles, but it remains uncertain how and to what extent the carbon and water cycles may change with WPE into grasslands under current climate. In this study, we examined the difference of vegetation indices (VIs), evapotranspiration (ET), gross primary production (GPP), and solar-induced chlorophyll fluorescence (SIF) during 2000–2010 between grasslands and juniper-encroached grasslands. We also quantitatively assessed the changes of GPP and ET for grasslands with different proportions of juniper encroachment (JWPE). Our results suggested that JWPE increased the GPP, ET, greenness-related VIs, and SIF of grasslands. Mean annual GPP and ET were, respectively, ~55% and ~45% higher when grasslands were completely converted into juniper forests under contemporary climate during 2000–2010. The enhancement of annual GPP and ET for grasslands with JWPE varied over years ranging from about +20% GPP (~+30% for ET) in the wettest year (2007) to about twice as much GPP (~+55% for ET) in the severe drought year (2006) relative to grasslands without encroachment. Additionally, the differences in GPP and ET showed significant seasonal dynamics. During the peak growing season (May–August), GPP and ET for grasslands with JWPE were ~30% and ~40% higher on average. This analysis provided insights into how and to what degree carbon and water cycles were impacted by JWPE, which is vital to understanding how JWPE and ecological succession will affect the regional and global carbon and water budgets in the future.

KEYWORDS: carbon cycle, drought, land cover, solar-induced chlorophyll fluorescence, vegetation index, water cycle, woody plant encroachment

1 INTRODUCTION

Grasslands and savannas constitute approximately 50% of the terrestrial land cover (Archer, 2010; Bailey, 1998). They account for about 30% of

terrestrial gross primary productivity (GPP) and play a critical role in global carbon and water cycles (Archer, 2010; Beer et al., 2010; Poulter et al., 2014). Over the past century, woody plants have been observed worldwide to be increasing in abundance and density in grasslands and savannas, a process termed “woody plant encroachment” (WPE; Archer, Vavra, Laycock, & Pieper, 1994; Archer, 2010; Scott, Jenerette, Potts, & Huxman, 2009). Ecological succession of grasslands to woodlands may alter ecosystem structure and function and can threaten ecosystem services (Msanne et al., 2017; Petrie, Collins, Swann, Ford, & Litvak, 2015). For example, an increase of woody plants in grasslands has been reported to alter animal habitats (Coppedge, Engle, Masters, & Gregory, 2004) and reduce biological diversity (Ratajczak, Nippert, & Collins, 2012; Van Els, Will, Palmer, & Hickman, 2010), forage, and livestock production (Anadon, Sala, Turner, & Bennett, 2014). The shift of a herbaceous ecosystem to a woody ecosystem has affected carbon (Mcculley & Jackson, 2012; O'Donnell & Caylor, 2012), water (Liu et al., 2016; Scott, Huxman, Williams, & Goodrich, 2006; Zou, Qiao, & Wilcox, 2016), nutrient (Liao et al., 2008; Mcculley, Archer, Boutton, Hons, & Zuberer, 2004), and biogeochemical cycles (Hibbard, Archer, Schimel, & Valentine, 2001; Hibbard, Schimel, Archer, Ojima, & Parton, 2003). In terms of the consequences of WPE on carbon and water cycles of grassland ecosystems, robust generalizations have not yet been made (Scott et al., 2014).

Semiarid ecosystems significantly influence the patterns of global carbon cycle (Poulter et al., 2014). Analyses on the U.S. carbon budget during the 1980s suggested that WPE across non-forest ecosystems may contribute to much of the net terrestrial carbon sink with an estimated range of ~23% to ~40% (Houghton, Hackler, & Lawrence, 1999; Pacala et al., 2001). However, this component of the carbon cycle has one of the largest uncertainties in the North American and global carbon budgets (Barger et al., 2011; Houghton, 2007). In recent decades, studies have been extensively conducted to examine the consequences of WPE on carbon pools and fluxes, including aboveground and belowground net primary production (ANPP, BNPP), aboveground biomass, and soil carbon pools using site observations, process-based models, and land use change models (Archer, Boutton, & Hibbard, 2001; Barger et al., 2011; Hughes et al., 2006; Jackson, Banner, Jobbagy, Pockman, & Wall, 2002; Knapp et al., 2008; Mcculley & Jackson, 2012; O'Donnell & Caylor, 2012). For example, some studies suggested that shrub or tree encroachment into mesic grasslands resulted in higher ANPP (Hughes et al., 2006; Knapp et al., 2008) and higher aboveground biomass (Asner, Archer, Hughes, Ansley, & Wessman, 2003; Asner & Martin, 2004; Mckinley & Blair, 2008). Eddy covariance (EC) flux measurements of woody encroachment at arid and semiarid grasslands of New Mexico and Arizona showed increased net ecosystem exchange of CO_2 (NEE) meaning enhanced carbon sequestration (Petrie et al., 2015; Scott et al., 2006). NEE can be partitioned into two components: gross primary

production (GPP) and ecosystem respiration (ER) (Beer et al., 2010). GPP is the amount of carbon dioxide fixed by vegetation, which is a critical component in the estimate of carbon sequestration (Damm et al., 2010; Gitelson et al., 2006; Lamberti & Steinman, 1997). To date, studies on the effects of WPE on GPP are restricted to field sites and are inadequate for understanding how WPE alters GPP in grasslands at broad landscape scales.

The effects of WPE on the water cycle have been considered a major concern because WPE can alter stream flow, groundwater recharge, and water yield (Archer, 2010). One of the major findings was that the effect of WPE on stream flow depends on the traits of woody plants and environment conditionals (e.g., climate, soil, and geomorphology; Archer, 2010; Huxman et al., 2005). Field experiments on water use of *Juniperus virginiana* (eastern redcedar) encroachment into a mesic prairie of central Oklahoma, USA, found that juniper encroachment reduced soil water content, stream flow, and groundwater recharge (Caterina, Will, Turton, Wilson, & Zou, 2014; Zou, Turton, Will, Engle, & Fuhlendorf, 2014). Evapotranspiration (ET) is a key eco-hydrological process linking water, energy, and carbon cycles (Jung et al., 2010). ET was observed to decrease by an average of 0.12 mm/day (~7% of daily ET) over three years following the removal of Ashe juniper (*Juniperus ashei*) compared to plots without juniper removal in an experiment conducted in northeastern Texas, USA (Dugas, Hicks, & Wright, 1998). Scott et al. (2006) compared ET of a riparian grassland, shrubland, and woodland in southeastern Arizona, USA, over 1 year using eddy flux measurements and found higher ET in areas with woody plant abundance. These site-level studies found a consistent increase of ET after WPE resultant of deep-rooted woody species replacing shallow-rooted herbaceous vegetation. However, the magnitude of increased ET due to WPE has not been quantified at landscape scale (Archer, 2010; Wine & Hendrickx, 2013).

Previous studies that explored the consequences of WPE on the carbon and water cycles were constrained to the plot or site scale and lasted for a short period (ranging from days to few years). Thus, there is a need for analyses at larger spatial and temporal scales. The availability of carbon and water flux products developed using remote sensing data allows us to examine changes in ecosystem function and vegetation over continuous spatial scales covering multiple consecutive years. This study aims to quantify the difference in GPP and ET for grasslands with juniper encroachment (JWPE) and grasslands without JWPE under semiarid and sub-humid climate in Oklahoma, USA. The specific objectives are to (a) examine the differences in GPP, ET, VIs, and SIF between grasslands with and without JWPE; (b) estimate the change ratios of GPP and ET by establishing a relationship between the differences of GPP and ET and the encroachment proportions of JWPE. We used GPP and ET products developed with Moderate-Resolution Imaging Spectroradiometer (MODIS) data and juniper forest encroachment maps generated from analyses of Landsat images during the period of 2000–

2010. Vegetation indices (VIs) and solar-induced fluorescence (SIF) were used as proxies of production to further understand the effects of WPE in grasslands on the carbon and water cycles. This study was implemented state-wide for the grasslands in Oklahoma, USA, which were widely encroached by juniper species in last several decades (Engle, Bidwell, & Moseley, 1996).

2 MATERIALS AND METHODS

2.1 Study area

Grasslands in Oklahoma (33.4°N–37.1°N, 94°W–103.2°W), USA, were selected as a study area because they have experienced and are undergoing extensive juniper encroachment (*Juniperus* spp.; JWPE), which is an evergreen tree species (Wang et al., 2018). Eastern redcedar (*J. virginiana*) is the primary encroaching species, followed by Ashe juniper (*J. ashei*). Other juniper species (*Juniperus pinchotii*, *Juniperus monosperma*, and *Juniperus scopulorum*) only occur sporadically (Engle et al., 1996). From east to west, the grasslands of Oklahoma consist of tallgrass, mixed-grass, and shortgrass prairie. The grasslands are distributed on various soil types with elevations from ~100-m to ~1,500-m above sea level. Grasslands in Oklahoma experience a temperate continental climate, with annual mean air temperature ranging from 13 to 17°C from north to south and an annual mean precipitation gradient from ~1,100-mm to ~400-mm from east to west. The grasslands experience highly variable annual precipitation in contrast to the annual mean air temperature (Supporting Information Figure S1).

2.2 Data

2.2.1 Land cover maps

We used the juniper forest maps for Oklahoma during 1984–2010 at 30-m spatial resolution, which were generated using a pixel- and phenology-based algorithm and PALSAR and Landsat images (Wang et al., 2017, 2018). These products were reported for five periods from the 1980s to 2000s including 1984–1989, 1990–1994, 1995–1999, 2000–2004, and 2005–2010 (Wang et al., 2018). They have an overall accuracy of about 96% and depict the historical distribution of juniper forests in Oklahoma (Wang et al., 2017, 2018). In this study, we used the juniper forest maps for the latest two periods: the early 2000s (2000–2004) and the late 2000s (2005–2010) to match the timeline of MODIS-based datasets. Then, a juniper forest map for 2000–2010 was generated by combining the maps of 2000–2004 and 2005–2010. These 30-m juniper forest maps of 2000–2004, 2005–2010, and 2000–2010 were binary (juniper forest or non-juniper forest) and were aggregated to 500-m (Figure 1, Supporting Information Figure S2a) and 0.5° (Supporting Information Figure S2c) spatial resolution, with the value of each pixel representing the percentage of juniper forest within that pixel. The aggregated juniper forest maps were then used for statistical analysis with

500-m GPP (VPM) (see Section 2.2.2), MODIS-based ET, vegetation indices (see Sections 2.2.3, 2.2.4), and solar-induced chlorophyll fluorescence (0.5°, see Section 2.2.5) data. We also used the 25-m PALSAR/Landsat-based forest map in 2010 generated by Qin et al. (2016) to describe the spatial distributions of non-juniper forests over the study area. In addition, this study used the MODIS land cover data (Collection 6) with 500-m spatial resolution (MCD12Q1) to document the annual dynamics of the grasslands in the study area from 2000 to 2010. We used the annual grassland layers and generated grassland maps in three study periods of 2000–2004, 2005–2010, and 2000–2010 by selecting the pixels with persistent grassland cover. The 500-m pure grassland maps were also resampled to 0.5° by calculating percent grasslands within each pixel to match SIF data.

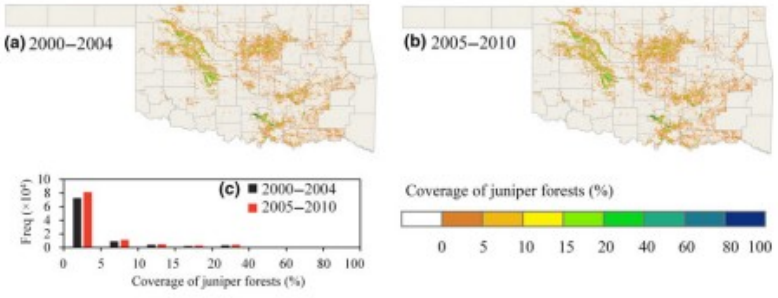

FIGURE 1 500-m juniper forest encroachment maps for (a) 2000–2004 and (b) 2005–2010; (c) the frequency histogram of juniper forest cover [Colour figure can be viewed at wileyonlinelibrary.com]

2.2.2 Gross primary production data

We used the 8-day GPP product simulated by the Vegetation Photosynthesis Model (VPM) for the period 2001–2010, which had a spatial resolution of 500-m (Zhang et al., 2016, 2017). The VPM is a light use efficiency model driven by remote sensing observations and climate data (Xiao et al., 2004). The GPP estimates from the VPM simulations have been validated for grasslands (GRA; Doughty et al., 2018; Wagle et al., 2014; Zhang et al., 2016, 2017; Zhou et al., 2017), woody savannas (WSA; Wang et al., 2016; Zhang et al., 2016, 2017), and savannas (SAV; Jin et al., 2013; Zhang et al., 2017) using eddy flux tower GPP (GPP_{EC}) data from around the globe (Supporting Information Table S1). A global accuracy assessment showed the R^2 and root-mean-square error (RMSE) of GPPvpm for GRA, WSA, and SAV were 0.79, 0.80, 0.70, and 1.2, 0.76, 0.7 gC m^{-2} day^{-1}, respectively. In Oklahoma, the R^2 and RMSE for GRA from the previous publications were 0.89 and 1.3 gC m^{-2} day^{-1} on average (Doughty et al., 2018; Wagle et al., 2014; Zhang et al., 2016; Zhou et al., 2017). The assessment of GPPvpm on the mesquite juniper woody savanna (US-FR2) in Texas, USA, showed a R^2 and RMSE of 0.73 and 1.13 gC m^{-2} day^{-1} using 3-year (2004–2006) 8-day data (Zhang et al., 2016). Overall, GPPvpm had consistent performance regardless of biome type when compared to GPP_{EC}.

2.2.3 Evapotranspiration data

We used the latest MODIS 8-day (MOD16A2, V06) and yearly (MOD16A3, V06) ET products with 500-m spatial resolution during 2001–2010. MOD16 ET is estimated using the Penman–Monteith equation, which considers the total evaporation of wet soil and canopy and plant transpiration (Mu, Zhao, & Running, 2013, 2011). The MODIS ET product has been widely used to analyze water flux over a variety of regions (Peng et al., 2014; Spera, Galford, Coe, Macedo, & Mustard, 2016). This study used the pixels with good observations as described by the quality layer. The average mean absolute biases (MAE) of daily ET for GRA and WSA were reported as 0.28 and 0.19 relative to AmeriFlux tower measurements (Mu et al., 2013; Running, Mu, Zhao, & Moreno, 2017; Supporting Information Table S2). Velpuri, Senay, Singh, Bohms, and Verdin (2013) comprehensively evaluated the MODIS ET data over the conterminous United States using FLUXNET tower data from 2001 to 2007 for various land cover types. The R^2 and RMSE of MODIS ET in GRA and WSA were reported as 0.41, 0.71, and 0.93, 0.63 mm/day, respectively (Supporting Information Table S2). In addition, we evaluated the performance of MODIS ET product for juniper cover by using the juniper mesquite WSA site (US-FR2, TX, USA; Heinsch et al., 2004). The mean R^2, RMSE, and MAE for juniper WSA were 0.78, 0.46, and 0.38 mm/day (Supporting Information Figure S3).

2.2.4 Vegetation index data

Normalized difference vegetation index (NDVI; Tucker, 1979), derived from optical remote sensing, is an indicator of vegetation greenness. In this study, we used the NDVI calculated from MODIS surface reflectance products (MOD09A1) with 500-m spatial resolution to delineate the canopy greenness of grasslands with and without JWPE.

2.2.5 Solar-induced chlorophyll fluorescence data

Solar-induced chlorophyll fluorescence (SIF) is emitted by plants simultaneously with photosynthesis. The satellite-based retrieval of SIF has created opportunities to remotely monitor photosynthesis and its dynamics at large spatial-temporal scales (Joiner et al., 2013; Zhang et al., 2018). Several studies have highlighted the strong relationship between SIF and GPP (Guanter et al., 2014; Jeong et al., 2017; Joiner et al., 2014; Yang et al., 2015). The SIF data products derived from NASA's Global Ozone Monitoring Instrument-2 (GOME-2) carried onboard the MetOP-A (launched in October 2006) and MetOP-B (launched in September 2012) satellites are available beginning in 2007 (https://acd-ext.gsfc.nasa.gov/People/Joiner/my_gifs/GOME_F/GOME-F.htm). This study used the Level 3 monthly gridded average data (GOME2_F version 27) from 2007 to 2010 with a spatial resolution of 0.5° to examine the potential physiological differences between grasslands with and without JWPE.

2.2.6 Climate data

We used a short-scale (6 months), monthly Standardized Precipitation Evapotranspiration Index (SPEI) with a 0.5° spatial resolution to document drought conditions for 2001–2010. SPEI is a climatic water balance-based drought index that considers the effects of precipitation and temperature variations on drought assessment, having a multi-scale character (Vicente-Serrano, Begueria, & Lopez-Moreno, 2010). SPEI was reported to perform well in capturing drought impacts on agriculture, ecology, and hydrology in a global assessment (Vicente-Serrano et al., 2012). This index has been widely used to examine the frequency, severity, and spatial-temporal changes of drought and other climatic characteristics (Paulo, Rosa, & Pereira, 2012; Yu, Li, Hayes, Svoboda, & Heim, 2014).

2.3 Statistical analysis on the effects of juniper encroachment in grasslands

2.3.1 Pairwise comparison between pure grasslands and juniper-encroached grasslands

To quantitatively understand the impacts of JWPE on grasslands in NDVI, ET, GPP, and SIF, we used the pairwise comparison approach with pure grassland (PG) pixels and juniper-encroached grassland (JEG) pixels, which necessitates that the PG and JEG pixels be adjacent. PG pixels were those with 100% coverage of grasslands, and JEG pixels were those with a certain percentage of juniper forests at any given pixel spatial resolution (e.g., 500-m, 0.5°). To match the spatial resolutions of the other datasets, the PG and JEG pixels were selected at two spatial resolutions, 500-m and 0.5° (~56-km), following these rules: (a) The samples of JEG should have relatively significant juniper forest cover; (b) the samples of adjacent PG should be covered by pure grasslands; and (c) the total vegetation cover between JEG pixels and adjacent PG pixels should be consistent. The adjacent PG pixels were selected from the neighborhood area of individual JEG pixels. The neighborhood window size was determined by considering two factors: (a) That enough PG pixels within the neighborhoods could be acquired and (b) that the window size reduces the influences of spatial heterogeneity on the results. Therefore, at 500-m spatial resolution, we used two sample windows of 11 × 11 (~5 × 5-km) and 21 × 21 (~10 × 10-km) pixels. For the coarser resolution of 0.5°, we only used a sample window of 3 × 3 pixels. Not all of the JEG pixels had adjacent PG pixels to constitute pairs for comparison, so this analysis was conducted by selecting the JEG pixels which have at least 10% adjacent PG pixels within the neighborhood windows of 3 × 3 (≥1 PG), 11 × 11 (≥12 PG), and 21 × 21 (≥44 PG) pixels.

During the selection of JEG pixels for constituting paired samples, we used juniper forest encroachment maps and the MODIS grassland maps at 500-m and 0.5°. At 500-m spatial resolution, the juniper forest encroachment maps were percentage of cover and grassland maps were binary (grassland or non-grassland). There is a chance of selecting JEG pixels only composed of juniper forests and grasslands without the cover of non-juniper forests at

500-m. To exclude the pixels with sparse JWPE, we used the JEG pixels having at least 10% juniper forest cover for both periods (2000–2004 and 2005–2010). This process also used the MODIS land cover maps during 2000–2010 and the PALSAR forest map in 2010 to control the sample quality. At 0.5° spatial resolution, there were no pure grassland pixels, and the percentage of juniper forests within each pixel was lower than 10% (Supporting Information Figure S2). Here, we only used the pixels with high vegetation coverage (>90%) instead and then selected the pixels as JEG samples that mainly consist of juniper forests and grasslands with juniper forest coverage higher than 2%. The corresponding adjacent grassland samples also had at least 90% grassland cover. The difference of total vegetation coverage between JEG and adjacent PG samples was within 5% at 0.5°. Finally, we, respectively, obtained 1,715 and 1 JEG samples at spatial resolutions of 500-m and 0.5° for the period of 2000–2010 (Supporting Information Figure S2b,d). Using these samples, we compared the annual mean GPP and ET and the seasonal dynamics of NDVI and SIF for grasslands with and without WPE.

2.3.2 The effects of JWPE on GPP and ET

The JEG pixels had various magnitudes of JWPE, which can be measured with juniper forest coverage. These magnitudes were not considered during the pairwise comparison analysis described in Section 2.3.1. The 500-m JWPE maps resampled from the 30-m products did not include any pure juniper forest pixels for either 2000–2004 or 2005–2010. Thus, the analysis was limited to the assessment of the differences in GPP and ET between pure juniper forest pixels and adjacent pure grassland pixels. Therefore, we created a conceptual framework (Supporting Information Figure S4) to quantify the differences in GPP and ET by combining the differences in GPP and ET with the proportion of JWPE within each pixel. Conceptually, the GPP and ET of a JEG pixel (GPP_{JEG}, ET_{JEG}) were composed of the flux of grasses (GPP_{grass}, ET_{grass}) and juniper forests (GPP_{JF}, ET_{JF}) within that pixel (Equations 1 and 2).

$$GPP_{JEG} = \alpha \times GPP_{JF} + (1-\alpha) \times GPP_{grass} \quad (1)$$

$$ET_{JEG} = \alpha \times ET_{JF} + (1-\alpha) \times ET_{grass} \quad (2)$$

Where GPP_{JEG} and ET_{JEG} denoted the actual GPP and ET of a given JEG pixel which can be obtained from the GPP and ET products directly. α was the fraction of juniper forests in the given JEG pixel. GPP_{JF} and ET_{JF} denoted the potential GPP and ET of the given JEG pixel under pure cover of juniper forests. $(1-\alpha)$ referred to the fraction of grasslands. GPP_{grass} and ET_{grass} were the potential GPP and ET of the given JEG pixel under pure cover of grasslands. In this model, we assumed that GPP_{JEG} (*or* ET_{JEG}) was a linear combination of GPP_{JF} (*or* ET_{JF}) and GPP_{grass} (*or* ET_{grass}) without considering the interactions between juniper forests and grasslands.

During the implementation of the model, we selected the 500-m JEG pixels for two periods of 2000–2004 and 2005–2010 using the sampling method described in Section 2.3.1 (Supporting Information Figure S5). We used Equations 1 and 2 at the individual pixel level for the two study periods to quantify the difference in GPP and ET for pixels with different ratios of grassland and juniper forest. Mathematically, Equation 1 or 2 can be transformed to Equations 3-5.

$$GPP_{JEG} - GPP_{grass} = \alpha \times (GPP_{JF} - GPP_{grass}) \quad (3)$$

$$\frac{GPP_{JEG} - GPP_{grass}}{GPP_{grass}} = \frac{\alpha \times (GPP_{JF} - GPP_{grass})}{GPP_{grass}} \quad (4)$$

$$\frac{(GPP_{JF} - GPP_{grass})}{GPP_{grass}} = \frac{\frac{GPP_{JEG} - GPP_{grass}}{GPP_{grass}}}{\alpha} \quad (5)$$

The left-side term of $(GPP_{JF} - GPP_{grass})/GPP_{grass}$ in Equation 5 quantifies the change in GPP when the grasslands in the given pixel were completely (100%) converted to juniper forests. We used the term *change ratio* (θ_{GPP}) to describe the expected change in GPP (Equation 6).

$$\theta_{GPP} = \frac{(GPP_{JF} - GPP_{grass})}{GPP_{grass}} \quad (6)$$

Following Equation 5, the left-side term can be estimated as the slope of a linear regression between the right-side terms of $(GPP_{JEG} - GPP_{grass})/GPP_{grass}$ and α based on all the selected pixels. Actually, $(GPP_{JEG} - GPP_{grass})/GPP_{grass}$ represented the change ratio of GPP when the grasslands in a given pixel were partially encroached by juniper forests with a proportion of α. Here, GPP_{JEG} can be obtained directly from GPP or ET products for each individual pixel. α was the corresponding coverage of juniper forests, which can be obtained from the juniper forest maps. We could not directly get the GPP of grassland (GPP_{grass}) within a pixel with juniper forest encroachment. Instead, we took the mean GPP of all adjacent PG pixels (GPP_{PGs}) within a neighborhood. In this study, we used neighborhoods with two sample windows of 11 × 11 pixels (~5-km) and 21 × 21 pixels (~10-km) at 500-m spatial resolution (see Section 2.3.1). Thus, the change ratio of GPP, θ_{GPP}, was assessed with the slope of a linear regression ($\frac{GPP_{JEG} - GPP_{grass}}{GPP_{grass}} \sim \alpha$) based on the selected JEG pixels and their adjacent PG pixels.

Evapotranspiration was analyzed using the same processes as GPP. Thus, the change ratio of ET (θ_{ET}) can be expressed as Equation 7, which can be estimated by a linear regression as described above.

$$\theta_{ET} = \left| \frac{(ET_{JF} - ET_{grass})}{ET_{grass}} \right| \quad (7)$$

The results of θ_{GPP} and θ_{ET} assessed based on the 11 × 11 sample window and the results using the 21 × 21 sample window are shown in Supporting Information. This analysis on θ_{GPP} and θ_{ET} was conducted at interannual and seasonal time scales during two periods of 2000–2004 and 2005–2010. In these two periods, θ_{GPP} and θ_{ET} were analyzed using the same model proposed in this study but different analysis samples due to different juniper forest and pure grassland maps. In the model, we used adjacent PG pixels as control for comparison to exclude the effects of environment factors on the changes of GPP and ET. θ_{GPP} and θ_{ET} were the change ratios of GPP and ET with grasslands entirely converted to juniper forests. We assumed that θ_{GPP} and θ_{ET} were primarily driven by vegetation change, so we expected consistent or similar θ_{GPP} and θ_{ET} calculated from the samples in different periods.

3 RESULTS

3.1 Pairwise comparisons of GPP, ET, NDVI, and SIF between JEG and PG

We compared mean annual GPP, ET, and the seasonal dynamics of NDVI and SIF of JEG and PG (Figure 2) pixels based on the samples shown in Supporting Information Figure S2. The higher GPP and ET values of JEG pixels suggested that JWPE increased annual GPP and ET of the grassland ecosystem (Figure 2a,b). The increases in GPP and ET vary between years. We found consistent patterns between JEG and PG in the seasonal dynamics of NDVI and SIF (Figure 2c,d). Higher NDVI demonstrated that JWPE could increase the greenness of the grassland ecosystem. Greater SIF indicated that the encroaching juniper had higher photosynthetic capacity than the native grasses at the chlorophyll level.

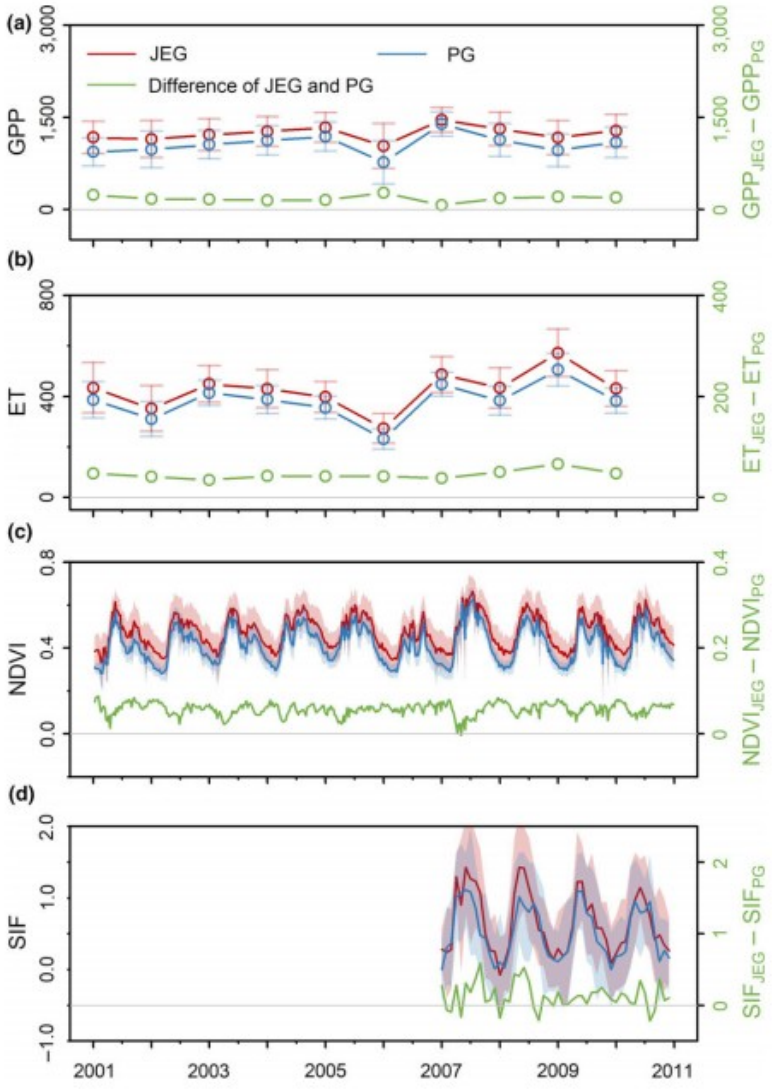

FIGURE 2 Comparisons of (a) annual gross primary production (GPP; gC m^{-2} $year^{-1}$); (b) annual evapotranspiration (ET; kg m^{-2} $year^{-1}$); (c) NDVI; and (d) solar-induced chlorophyll fluorescence (SIF; mW m^{-2} nm^{-1} sr^{-1}) between pure grasslands (PG) and juniper-encroached grassland (JEG). The figures also show the difference of each variable between JEG and PG. The standard deviation (*SD*) for each variable is shown in the figure by error bars (a, b) and shadows (c, d) [Colour figure can be viewed at wile yonlinelibrary.com]

3.2 The change ratios of GPP and ET estimated from multi-year mean annual data

The change ratios of GPP and ET (θ_{GPP} and θ_{ET}) were estimated using our conceptual model (Equations 1 and 2), which was based on the pairwise comparison of multi-year mean annual GPP and ET between JEG and PG pixels the periods 2000–2004 and 2005–2010 (Supporting Information Figure S5). The results are shown in Figure 3. All the regressions in Figure 3a–d are significant with $p < 0.001$. From the slopes of the linear regressions, θ_{GPP} was 0.59 (59%) and 0.55 (55%), and θ_{ET} was 0.43 (43%) and 0.45 (45%) in 2000–2004 and 2005–2010, respectively. These results suggested that GPP would increase by about 55%–59% and the ET would increase by about 43%–45% if the grasslands in the study area were 100% converted to juniper forests under contemporary 2000–2010 environmental conditions. The results shown in Figure 3 were calculated with a neighborhood window of 11 × 11 pixels.

We obtained similar results at the neighborhood window of 21 × 21 pixels (Supporting Information Figure S6). The carbon and water budgets for juniper woody encroachment can be estimated using this result. For example, mean annual GPP and ET of grasslands without JWPE were about 990 ± 200, 1060 ± 210 gC m^{-2} $year^{-1}$, and 367 ± 45, 380 ± 37 kg m^{-2} $year^{-1}$ for 2000–2004 and 2005–2010, respectively (Figure 3e). According to the 500-m juniper woody map in 2005–2010, the estimated mean juniper coverage in the study area was ~4.5% with a total area of ~2.6 × 10^4-km^2 (Figure 1b). The ~4.5% JWPE into the grasslands in Oklahoma could have caused the ecosystem to uptake an additional carbon of 8.7 × 10^{11} gC/year with extra water loss of 1.9 × 10^{11} kg/year by ET.

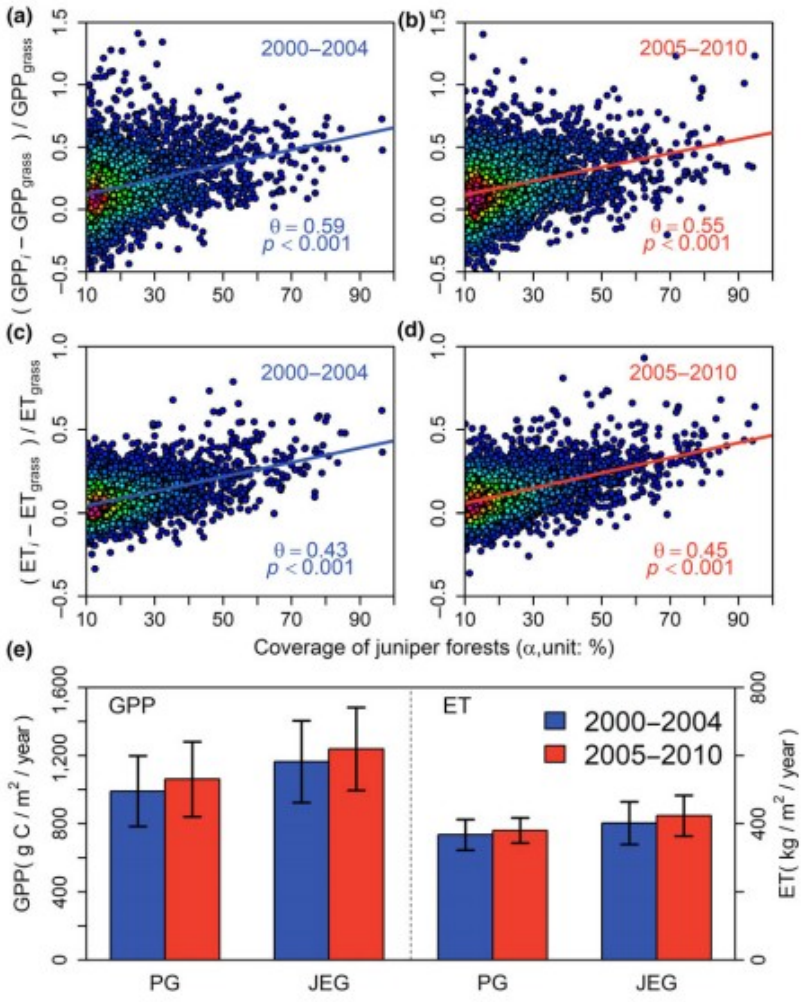

FIGURE 3 Linear regressions of change ratios of GPP (a, b) and ET (c, d) with juniper forest coverage based on the selected juniper-encroached grassland (JEG) samples and their adjacent pure grassland (PG) pixels within a neighborhood window of 11 × 11 pixels (see Supporting Information Figure S5a,b). The number of JEG samples was 3,630 and 4,398 in 2000–2004 and 2005–2010, respectively. This analysis used multi-year mean annual GPP and ET, and juniper forest encroachment maps during 2000–2004 and 2005–2010. The slope (θ) describes the change ratio of GPP or ET with grasslands entirely converted to juniper forests. (e) shows multi-year mean annual GPP and ET of the native grasslands and juniper-encroached grasslands for two periods [Colour figure can be viewed at wileyonlinelibrary.com]

3.3 Interannual variations of the change ratios of GPP and ET during 2001–2010

Grasses and woody plants responded differently to the interannual variations in precipitation and temperature (Figure 2a,b), so the change ratios of GPP and ET were expected to vary under different climate conditions. Here, we examined the interannual variations of the change ratios of GPP and ET

(θ_{GPP} and θ_{ET}) over the period of 2001–2010 using annual GPP and ET data (Figure 4). Corresponding linear regressions for calculating θ_{GPP} and θ_{ET} are shown in Supporting Information Figure S7. θ_{GPP} ranged from 0.2 to 2.1 with the maximum and minimum values occurring in 2006 and 2007, respectively. θ_{ET} varied from 0.31 to 0.59. The maximum and minimum values also occurred in the years of 2006 and 2007. As hydrological conditions have obvious interannual variations in semiarid regions, we plotted the 6-month SPEI during 2001–2010 in Figure 4a to examine the effects of water stress on θ_{GPP} and θ_{ET}. SPEI showed that 2006 was the driest year and 2007 was the wettest year. We calculated the mean annual SPEI and fitted the relationships of θ_{GPP} and SPEI (Figure 4b), and θ_{ET} and SPEI (Figure 4c). These relationships were significant with $p < 0.01$. These results demonstrated that the change ratios of GPP and ET (θ_{GPP} and θ_{ET}) caused by JWPE would be higher in a dry climate condition (e.g., 2006) than in a wet climate condition (e.g., 2007). Our results were consistent when using the JWPE pixels selected at the neighborhood window of 21 × 21 pixels (Supporting Information Figure S8).

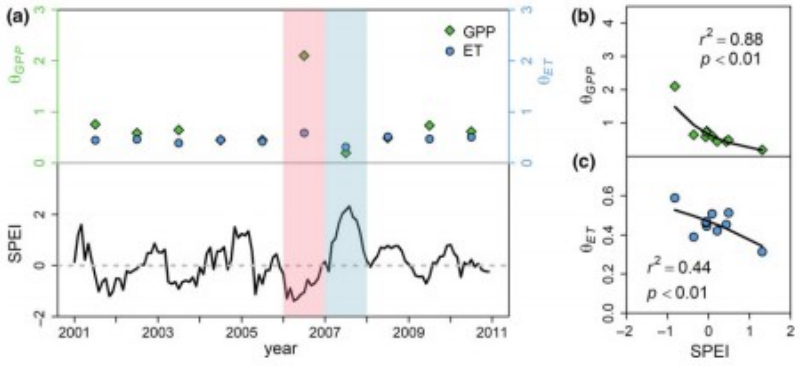

FIGURE 4 (a) Interannual dynamics of the change ratios of GPP (θ_{GPP}) and ET (θ_{ET}) with grasslands converted into juniper forests. The corresponding linear regressions are shown in Supporting Information Figure S7. Time series of Standardized Precipitation Evapotranspiration Index (SPEI) at 6-month scale is also exhibited to show the hydrological condition of each year. (b) The relationship of θ_{GPP} and annual mean SPEI. (c) The relationship of θ_{ET} and annual mean SPEI. This analysis was based on the juniper-encroached grassland pixels and their adjacent pure grasslands within a neighborhood window of 11 × 11 pixels (Supporting Information Figure S5a,b) [Colour figure can be viewed at wileyonlinelibrary.com]

3.4 Seasonal dynamics of the change ratios of GPP and ET

Evergreen juniper species have different phenology than grasses, which may cause the seasonal differences in GPP and ET between juniper forests and grasslands. Figure 5a shows the seasonality of θ_{GPP} and θ_{ET} calculated from the mean monthly GPP and ET data during 2001–2010. The linear regressions for each month are shown in Supporting Information Figures S9 and S10. The values of monthly θ_{GPP} were higher than 1.0 during the period from the late fall (November) to the middle spring (April), and were especially high in winter. These values drop dramatically from late spring (May) to mid-fall (October), which were <1.0. The lowest values of about 0.2 occurred in the peak grow season of June and July. Compared with θ_{GPP}, θ_{ET} showed a different seasonality. The lowest values, from −0.01 to 0.01, happen in winter, which demonstrated that ET from woody plants

was comparable with that from grasslands during this time. θ_{ET} had high values larger than 0.3 during the growing season from April to October. Figure 5a,b also shows the seasonality of mean monthly GPP and ET for grasslands. In winter, grasslands had negligible GPP and very low ET (<1 kg m^{-2} day^{-1}). From April to October, the photosynthesis of native grassland was above 1 gC m^{-2} day^{-1}. The GPP and ET of grasslands peaked in May and June with a maximum of about 6 gC m^{-2} day^{-1} and 2 kg m^{-2} day^{-1}, respectively. Similar results were obtained using the neighborhood window of 21 × 21 pixels (Supporting Information Figure S11). To explain the seasonal dynamics of θ_{GPP} and θ_{ET}, we examined the seasonal dynamics of NDVI for juniper forests and grasslands from two samples (Supporting Information Figure S12) and the mean monthly temperature and precipitation during 2001–2010 (Figure 5c). Figure 5c shows that the NDVI of juniper forests was higher than that of grasslands in winter and becomes comparable in peak growing season. The mean temperature in winter was above 0°C (Figure 5c). We also examined the average winter GPP using the flux tower measurements for one juniper woodland site (US-FR2) and three grassland sites of US-AR1, US-AR2, and US-ARc (Supporting Information Figure S13). The tower-based results showed the average GPP of juniper woodland was ~1.31 gC m^{-2} day^{-1} greater than the grassland GPP of ~0.16 gC m^{-2} day^{-1}, suggesting that juniper forests can have photosynthesis during the winter time (if environmental conditions were favorable) while grassland was dormant. This seasonal difference in photosynthetic activity produces the large change ratios of θ_{GPP} and θ_{ET} in winter.

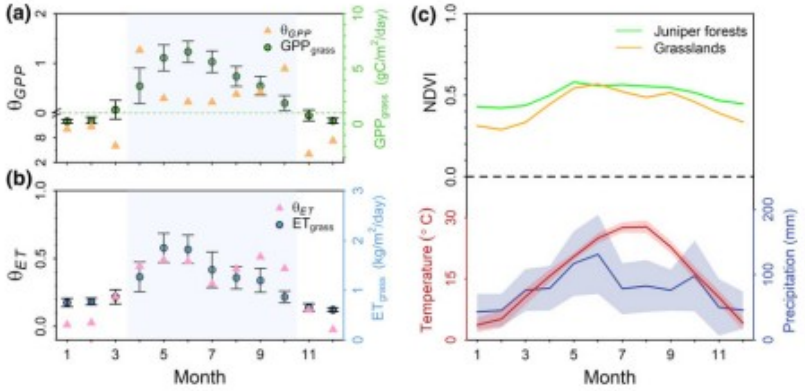

FIGURE 5 (a, b) Seasonal dynamics of the change ratios of GPP (θ_{GPP}) and ET (θ_{ET}) with grasslands converted into juniper forests based on mean monthly GPP and ET during 2001–2010. The corresponding linear regressions for each month are shown in Supporting Information Figures S9 and S10. Additionally, these figures show the mean monthly GPP and ET for the grasslands. The months with obvious photosynthesis (>1 gC m^{-2} day^{-1} shown by the dash line in Figure 5a) in grasslands are shown in shadows. (c) The seasonal dynamics of NDVI at two samples of juniper forests and pure grasslands extracted from 500-m MODIS data. The landscapes for the samples are shown in Supporting Information Figure S12 using Google Earth images. This figure also shows the mean monthly temperature and precipitation over the period of 2000–2010. This analysis was based on the juniper-encroached grassland pixels and their adjacent pure grasslands within a neighborhood window of 11 × 11 pixels (Supporting Information Figure S5a,b) [Colour figure can be viewed at wileyonlinelibrary.com]

4 DISCUSSION

4.1 Estimates of the change ratios of GPP and ET

Understanding how alterations in ecosystem species composition affect biogeochemical cycles provides insights into predicting the climate in the future (Chapin et al., 1997). This study established a model based on an assumption of total vegetation conversion from grasslands to juniper forest, which allowed for quantitatively assessing the changes of GPP and ET caused by JWPE under contemporary environmental conditions during 2000–2010. The challenge of this method was to acquire the GPP and ET values for each individual pixel before JWPE. Therefore, we used the mean GPP and ET obtained from adjacent PG pixels to approximate what GPP and ET would have been for each individual JEG pixel before JWPE. A small neighborhood size would not provide an adequate number of PG pixels for analysis, and a large neighborhood may be influenced by spatial heterogeneity, so this study used two sample window sizes, 11 × 11 and 21 × 21 pixels. We found that the results from 21 × 21 neighborhood window (Supporting Information Figures S6, S8 and S11) were consistent with the results obtained from 11 × 11 window (Figures 3–5-3–5). This approach of using grid cells to select adjacent biomes has been widely used to study the ecological consequences of land cover change (Ma, Jia, & Zhang, 2017; Peng et al., 2014). Additionally, this study used the MODIS-based GPP and ET products. Some uncertainties in the estimates of the change ratios of GPP (θ_{GPP}) and ET (θ_{ET}) could be caused by the performance of these products. The uncertainty analysis in previous publications and this work suggested that both datasets have reasonable accuracy for application in the GRA and juniper WSA biomes of Oklahoma, USA (Supporting Information Tables S1 and S2, and Supporting Information Figure S3). Here, we used the juniper WSA site (US-FR2) in Texas, USA, as an alternative way to evaluate the uncertainty of GPPvpm and MODIS ET products for juniper WSA in our study area. It was practical because this site was in the same Köppen-Geiger climate zone as Oklahoma (Peel, Finlayson, & Mcmahon, 2007) and it has similar annual precipitation and annual mean temperature. From this accuracy assessment and the results from previous studies (Mildrexler, Yang, Cohen, & Bell, 2016; Peng et al., 2014; Zhang et al., 2016), we used the datasets with confidence for our analyses.

The results suggested that had all grasslands been converted to juniper forest due to JWPE, annual GPP and ET would have been ~54% and ~44% higher during 2000–2010, respectively (Figure 3, Supporting Information Figure S6). Although direct estimates of GPP and ET dynamics of mesic tall- and mixed-grasslands caused by JWPE based on satellite observations are few, some similar studies have been conducted using flux tower observations or field measurements to survey the impacts of woody encroachment (Dugas et al., 1998; Jenerette, Scott, Barron-Gafford, & Huxman, 2009; Petrie et al., 2015; Scott et al., 2006). Qiao, Zou, Will, and Stebler (2015) reported that eastern redcedar encroached grasslands, on average, had 100-mm higher annual ET than the pure grasslands in

Oklahoma by using the Soil and Water Assessment Tool (SWAT model) and experimental measurements during 2011–2013. Scott et al. (2006) founded that ET increased with the density of woodland by eddy covariance observations in riparian woodland and grassland communities in southern Arizona. Jenerette et al. (2009) examined 3 years of data from the same sites and found that the woodland site had higher GPP than did the grassland site. A longer-term study using 5 years of flux tower measurements in southern Arizona also found that the riparian woodlands had much greater gross carbon uptake (GEP) and ET than adjacent grasslands (Scott et al., 2014). According to the flux tower data around riparian sites from 2003 to 2007, mean annual GEP and mean annual ET of the woodland site were 34% and 26% higher than those of the grassland site (Scott et al., 2014). In this previous study, the woodland site was dominated by mesquite with 70% canopy cover. The results of our study showed higher values of GPP and ET due to encroachment, but we focused on grasslands that had been entirely encroached (100%) by juniper. In addition, previous studies found that the grassland site with WPE had a higher water use efficiency (WUE) than the nearby grassland site, especially at seasonal and annual timescales, in a native tallgrass prairie in Kansas, USA (Brunsell, Nippert, & Buck, 2014; Logan & Brunsell, 2015). Our results showed that the change ratios of annual GPP (~54%) are higher than that of annual ET (~44%) when juniper forests replaced the grasslands entirely (Figure 3), which corroborated previous findings of enhanced WUE by WPE. However, further direct measurements and analysis are needed to better understand how WUE changes due to WPE. These analyses showed our results are very similar to those reported by site-specific studies on woody plant encroachment.

4.2 Interpretations for annual and seasonal dynamics of the change ratios of GPP and ET

This study indicated that in dry conditions (2006), the difference in GPP and ET between pure grasslands and those with JWPE was greater than in pluvial conditions (2007) (Figure 4). Many studies have reported that decreases in carbon sequestration of grasslands were associated with decreased precipitation (Bowling, Bethers-Marchetti, Lunch, Grote, & Belnap, 2010; Schwalm et al., 2010). In dry years, many grasslands have been found to shift from being a carbon sink to a carbon source (Aires, Pio, & Pereira, 2008; Petrie et al., 2015), even though the WPE grasslands may have this switch when the encroaching species cannot use additional water resources (Scott, Biederman, Hamerlynck, & Barron-Gafford, 2015). Woody plants have deeper roots than grasses and can access deep soil moisture and even ground water (Archer et al., 2001; Ratajczak, Nippert, Hartman, & Ocheltree, 2011; Wang et al., 2016). For example, a study on a riparian woodland suggested the groundwater access increased the net ecosystem production (NEP) and ET in comparison with the surrounding upland areas (Scott et al., 2014). According to these results, we may expect significant increases in GPP and ET with WPE when the additional water resources of deep soil water or groundwater are

available for trees compared to that of the grasses with limited access to deeper layer soil moisture. Encroaching woody plants are expected to have a lower sensitivity to precipitation variability and a higher resistance and resilience to drought than grasses (Logan & Brunsell, 2015; Scott et al., 2014). Our results support this statement, because GPP and ET for juniper-encroached grasslands were greater than those of pure grasslands (Figure 2). During the dry year, the GPP and ET of JEG and PG fell but the reduction of GPP and ET was higher for PG than JEG (Figure 2). This difference resulted in larger change ratios of GPP and ET (Figure 4). On the other hand, in the pluvial year of 2007, the increases of GPP and ET in PG were similar to or greater than those in JEG (Figure 2), which resulted in smaller differences of GPP and ET between JEG and PG (Figure 4). Thus, the change ratios of GPP and ET were low in the pluvial condition than those of drought condition. Eastern redcedar is a species tolerant to drought (Msanne et al., 2017) and can maintain photosynthesis at low water potentials (Eggemeyer, Awada, Wedin, Harvey, & Zhou, 2006; Willson, Manos, & Jackson, 2008). Under low water availability, eastern redcedar can access the deep soil water and their roots can reach a depth of up to 7 m (Msanne et al., 2017). These traits enable eastern redcedar to successfully encroach arid and semiarid grasslands (Msanne et al., 2017). The ability of juniper trees to access water resources deeper in the soil profile than grasses could potentially explain the different responses of GPP and ET (θ_{GPP} and θ_{ET}) in the dry and pluvial year of 2006 and 2007. Some similar results were reported in previous studies. Petrie et al. (2015) found that drier than average climate conditions facilitated increases in terrestrial carbon sequestration caused by the vegetation conversion from grasslands to shrublands. Logan and Brunsell (2015) reported carbon flux at a woody site was double or more than triple that of a grassland site during wet years, while the difference became remarkably large under drought conditions.

Our study shows different seasonal dynamics of the change ratios of GPP (θ_{GPP}) and ET (θ_{ET}) with maximum θ_{GPP} in winter and maximum θ_{ET} in growing season (Figure 5). Despite low temperature and precipitation in winter, the GPP of juniper forest was much higher (about tenfold) relative to the grassland ecosystem during this period (Figure 5). Juniper species are evergreen and have higher NDVI than grasslands in winter (Figures 2c and 5c). Thus, juniper trees can continue to photosynthesize during winter if temperatures and water are favorable while grasslands are dormant (Supporting Information Figure S13). During the growing season, especially from May to September, the difference in NDVI between grasslands and juniper forests was relatively negligible. Likewise, the low θ_{GPP} (from 0.22 to 0.42) in this period signals that both grasslands and juniper forest are highly productive. In winter, θ_{ET} was around zero (Figure 5), which indicated that ecological succession of grasslands to juniper forests would not significantly increase ET during this period. However, in the growing season, this vegetation conversion would produce a ~30%–50% increase in ET

(Figure 5, Supporting Information Figure S10). It is consistent with an early study on a riparian region, which showed woodlands had ~57% higher ET than grasslands during the growing season (Scott et al., 2006). As deep-rooted trees can acquire deep soil moisture or groundwater and grasslands depend on precipitation or topsoil moisture, the ability of trees to acquire water deeper in the soil profile likely supports the higher ET observed in grasslands with WPE (Scott et al., 2006).

ACKNOWLEDGEMENTS

This study was supported by research grants through the USDA National Institute of Food and Agriculture (NIFA) (2013-69002 and 2016-68002-24967) and the US National Science Foundation EPSCoR program (IIA-1301789). This work used the Fluxnet2015 eddy covariance dataset acquired and shared by the FLUXNET community, including these networks: AmeriFlux, AfriFlux, AsiaFlux, CarboAfrica, CarboEuropeIP, CarboItaly, CarboMont, ChinaFlux, Fluxnet-Canada, GreenGrass, ICOS, KoFlux, LBA, NECC, OzFlux-TERN, TCOS-Siberia, and USCCC. We thank anonymous reviewers for their insightful and constructive comments and suggestions on the earlier version of the manuscript.

References

Aires, L. M. I., Pio, C. A., & Pereira, J. S. (2008). Carbon dioxide exchange above a Mediterranean C3/C4 grassland during two climatologically contrasting years. *Global Change Biology*, 14, 539– 555. https://doi.org/10.1111/j.1365-2486.2007.01507.x

Anadon, J. D., Sala, O. E., Turner, B. L., & Bennett, E. M. (2014). Effect of woody-plant encroachment on livestock production in North and South America. *Proceedings of the National Academy of Sciences of the United States of America*, 111, 12948– 12953. https://doi.org/10.1073/pnas.1320585111

Archer, S. R. (2010). Rangeland conservation and shrub encroachment: New perspectives on an old problem. In J. T. Toit, R. Kock, & J. C. Deutsch (Eds.), *Wild rangelands: Conserving wildlife while maintaining livestock in semi-arid ecosystems* (pp. 53– 97). Oxford, UK: Wiley-Blackwell. https://doi.org/10.1002/9781444317091

Archer, S., Boutton, T. W., & Hibbard, K. A. (2001). Trees in grasslands: Biogeochemical consequences of woody plant expansion. In E.-D. Schulze, S. P. Harrison, M. Heimann, E. A. Holland, J. Lloyd, I. C. Prentice, & D. Schimel (Eds.), *Global biogeochemical cycles in the climate system* (pp. 115– 138). Cambridge, CA: Academic Press. https://doi.org/10.1016/B978-012631260-7/50011-X

Archer, S., Vavra, M., Laycock, W., & Pieper, R. (1994). Woody plant encroachment into southwestern grasslands and savannas: Rates, patterns and proximate causes. In M. Vavra, W. A. Laycock, & R. D.

Pieper (Eds.), *Ecological implications of livestock herbivory in the west* (pp. 13– 68). Denver, CO: Society for Range Management.

Asner, G. P., Archer, S., Hughes, R. F., Ansley, R. J., & Wessman, C. A. (2003). Net changes in regional woody vegetation cover and carbon storage in Texas Drylands, 1937–1999. *Global Change Biology*, 9, 316– 335. https://doi.org/10.1046/j.1365-2486.2003.00594.x

Asner, G. P., & Martin, R. E. (2004). Biogeochemistry of desertification and woody encroachment in grazing systems. *Ecosystems and Land Use Change*, 153, 99– 116. https://doi.org/10.1029/GM153

Bailey, R. G. (1998). *Ecoregions*. Berlin, Germany: Springer. https://doi.org/10.1007/978-1-4612-2200-2

Barger, N. N., Archer, S. R., Campbell, J. L., Huang, C. Y., Morton, J. A., & Knapp, A. K. (2011). Woody plant proliferation in North American drylands: A synthesis of impacts on ecosystem carbon balance. *Journal of Geophysical Research-Biogeosciences*, 116, G00k07.

Beer, C., Reichstein, M., Tomelleri, E., Ciais, P., Jung, M., Carvalhais, N., … Papale, D. (2010). Terrestrial gross carbon dioxide uptake: Global distribution and covariation with climate. *Science*, 329, 834– 838. https://doi.org/10.1126/science.1184984

Bowling, D. R., Bethers-Marchetti, S., Lunch, C. K., Grote, E. E., & Belnap, J. (2010). Carbon, water, and energy fluxes in a semiarid cold desert grassland during and following multiyear drought. *Journal of Geophysical Research-Biogeosciences*, 115, G04026.

Brunsell, N. A., Nippert, J. B., & Buck, T. L. (2014). Impacts of seasonality and surface heterogeneity on water-use efficiency in mesic grasslands. *Ecohydrology*, 7, 1223– 1233.

Caterina, G. L., Will, R. E., Turton, D. J., Wilson, D. S., & Zou, C. B. (2014). Water use of *Juniperus virginiana* trees encroached into mesic prairies in Oklahoma, USA. *Ecohydrology*, 7, 1124– 1134.

Chapin, F. S., Walker, B. H., Hobbs, R. J., Hooper, D. U., Lawton, J. H., Sala, O. E., & Tilman, D. (1997). Biotic control over the functioning of ecosystems. *Science*, 277, 500– 504. https://doi.org/10.1126/science.277.5325.500

Coppedge, B. R., Engle, D. M., Masters, R. E., & Gregory, M. S. (2004). Predicting juniper encroachment and CRP effects on avian community dynamics in southern mixed-grass prairie, USA. *Biological Conservation*, 115, 431– 441. https://doi.org/10.1016/S0006-3207(03)00160-5

Damm, A., Elbers, J., Erler, A., Gioli, B., Hamdi, K., Hutjes, R., … Rascher, U. (2010). Remote sensing of sun-induced fluorescence to improve modeling

of diurnal courses of gross primary production (GPP). *Global Change Biology*, 16, 171– 186. https://doi.org/10.1111/(ISSN)1365-2486

Doughty, R., Xiao, X., Wu, X., Zhang, Y., Bajgain, R., Zhou, Y., … Steiner, J. (2018). Responses of gross primary production of grasslands and croplands under drought, pluvial, and irrigation conditions during 2010–2016, Oklahoma, USA. *Agricultural Water Management*, 204, 47– 59. https://doi.org/10.1016/j.agwat.2018.04.001

Dugas, W. A., Hicks, R. A., & Wright, P. (1998). Effect of removal of *Juniperus ashei* on evapotranspiration and runoff in the Seco Creek watershed. *Water Resources Research*, 34, 1499– 1506. https://doi.org/10.1029/98WR00556

Eggemeyer, K. D., Awada, T., Wedin, D. A., Harvey, F. E., & Zhou, X. H. (2006). Ecophysiology of two native invasive woody species and two dominant warm-season grasses in the semiarid grasslands of the Nebraska Sandhills. *International Journal of Plant Sciences*, 167, 991– 999. https://doi.org/10.1086/505797

Engle, D. M., Bidwell, T. G., & Moseley, M. E. (1996). *Invasion of Oklahoma rangelands and forests by Eastern Redcedar and Ashe Juniper*. Stillwater, OK: Oklahoma Cooperative Extension Service, Division of Agricultural Sciences and Natural Resources, Oklahoma State University.

Gitelson, A. A., Vina, A., Verma, S. B., Verma, S. B., Rundquist, D. C., Arkebauer, T. J., … Suyker, A. E. (2006). Relationship between gross primary production and chlorophyll content in crops: Implications for the synoptic monitoring of vegetation productivity. *Journal of Geophysical Research-Atmospheres*, 111, D8.

Guanter, L., Zhang, Y., Jung, M., Joiner, J., Voigt, M., Berry, J. A., … Griffis, T. J. (2014). Global and time-resolved monitoring of crop photosynthesis with chlorophyll fluorescence. *Proceedings of the National Academy of Sciences of the United States of America*, 111, E1327– E1333. https://doi.org/10.1073/pnas.1320008111

Heinsch, F. A., Heilman, J. L., Mcinnes, K. J., Cobos, D. R., Zuberer, D. A., & Roelke, D. L. (2004). Carbon dioxide exchange in a high marsh on the Texas Gulf Coast: Effects of freshwater availability. *Agricultural and Forest Meteorology*, 125, 159– 172. https://doi.org/10.1016/j.agrformet.2004.02.007

Hibbard, K., Archer, S., Schimel, D., & Valentine, D. (2001). Biogeochemical changes accompanying woody plant encroachment in a subtropical savanna. *Ecology*, 82, 1999– 2011. https://doi.org/10.1890/0012-9658(2001)082[1999:BCAWPE]2.0.CO;2

Hibbard, K. A., Schimel, D. S., Archer, S., Ojima, D. S., & Parton, W. (2003). Grassland to woodland transitions: Integrating changes in landscape structure and biogeochemistry. *Ecological Applications*, 13, 911– 926. https://doi.org/10.1890/1051-0761(2003)13[911:GTWTIC]2.0.CO;2

Houghton, R. A. (2007). Balancing the global carbon budget. *Annual Review of Earth and Planetary Sciences*, 35, 313– 347. https://doi.org/10.1146/annurev.earth.35.031306.140057

Houghton, R. A., Hackler, J. L., & Lawrence, K. T. (1999). The US carbon budget: Contributions from land-use change. *Science*, 285, 574– 578. https://doi.org/10.1126/science.285.5427.574

Hughes, R. F., Archer, S. R., Asner, G. P., Wessman, C. A., Mcmurtry, C., Nelson, J., & Ansley, R. J. (2006). Changes in aboveground primary production and carbon and nitrogen pools accompanying woody plant encroachment in a temperate savanna. *Global Change Biology*, 12, 1733– 1747. https://doi.org/10.1111/j.1365-2486.2006.01210.x

Huxman, T. E., Wilcox, B. P., Breshears, D. D., Scott, R. L., Snyder, K. A., Small, E. E., … Jackson, R. B. (2005). Ecohydrological implications of woody plant encroachment. *Ecology*, 86, 308– 319. https://doi.org/10.1890/03-0583

Jackson, R. B., Banner, J. L., Jobbagy, E. G., Pockman, W. T., & Wall, D. H. (2002). Ecosystem carbon loss with woody plant invasion of grasslands. *Nature*, 418, 623– 626. https://doi.org/10.1038/nature00910

Jenerette, G. D., Scott, R. L., Barron-Gafford, G. A., & Huxman, T. E. (2009). Gross primary production variability associated with meteorology, physiology, leaf area, and water supply in contrasting woodland and grassland semiarid riparian ecosystems. *Journal of Geophysical Research-Biogeosciences*, 114, G04010.

Jeong, S. J., Schimel, D., Frankenberg, C., Drewry, D. T., Fisher, J. B., Verma, M., … Joiner, J. (2017). Application of satellite solar-induced chlorophyll fluorescence to understanding large-scale variations in vegetation phenology and function over northern high latitude forests. *Remote Sensing of Environment*, 190, 178– 187. https://doi.org/10.1016/j.rse.2016.11.021

Jin, C., Xiao, X. M., Merbold, L., Arneth, A., Veenendaal, E., & Kutsch, W. L. (2013). Phenology and gross primary production of two dominant savanna woodland ecosystems in Southern Africa. *Remote Sensing of Environment*, 135, 189– 201. https://doi.org/10.1016/j.rse.2013.03.033

Joiner, J., Guanter, L., Lindstrot, R., Voigt, M., Vasilkov, A. P., Middleton, E. M., … Frankenberg, C. (2013). Global monitoring of terrestrial chlorophyll fluorescence from moderate-spectral-resolution near-infrared satellite measurements: methodology, simulations, and application to GOME-2. *Atmospheric Measurement Techniques*, 6, 2803– 2823. https://doi.org/10.5194/amt-6-2803-2013

Joiner, J., Yoshida, Y., Vasilkov, A. P., Schaefer, K., Jung, M., Guantere, L., … Belelli Marchesini, L. (2014). The seasonal cycle of satellite chlorophyll

fluorescence observations and its relationship to vegetation phenology and ecosystem atmosphere carbon exchange. *Remote Sensing of Environment*, 152, 375– 391. https://doi.org/10.1016/j.rse.2014.06.022

Jung, M., Reichstein, M., Ciais, P., Seneviratne, S. I., Sheffield, J., Goulden, M. L., … Zhang, K. (2010). Recent decline in the global land evapotranspiration trend due to limited moisture supply. *Nature*, 467, 951– 954. https://doi.org/10.1038/nature09396

Knapp, A. K., Briggs, J. M., Collins, S. L., Archer, S. R., Bret-Harte, M. S., Ewers, B. E., … Cleary, M. B. (2008). Shrub encroachment in North American grasslands: Shifts in growth form dominance rapidly alters control of ecosystem carbon inputs. *Global Change Biology*, 14, 615– 623. https://doi.org/10.1111/j.1365-2486.2007.01512.x

Lamberti, G. A., & Steinman, A. D. (1997). A comparison of primary production in stream ecosystems. *Journal of the North American Benthological Society*, 16, 95– 104. https://doi.org/10.2307/1468241

Liao, C. Z., Peng, R. H., Luo, Y. Q., Zhou, X., Wu, X., Fang, C., … Li, B. (2008). Altered ecosystem carbon and nitrogen cycles by plant invasion: A meta-analysis. *New Phytologist*, 177, 706– 714. https://doi.org/10.1111/j.1469-8137.2007.02290.x

Liu, Y. B., Xiao, J. F., Ju, W. M., Xu, K., Zhou, Y. L., & Zhao, Y. T. (2016). Recent trends in vegetation greenness in China significantly altered annual evapotranspiration and water yield. *Environmental Research Letters*, 11, 094010. https://doi.org/10.1088/1748-9326/11/9/094010

Logan, K. E., & Brunsell, N. A. (2015). Influence of drought on growing season carbon and water cycling with changing land cover. *Agricultural and Forest Meteorology*, 213, 217– 225. https://doi.org/10.1016/j.agrformet.2015.07.002

Ma, W., Jia, G. S., & Zhang, A. Z. (2017). Multiple satellite-based analysis reveals complex climate effects of temperate forests and related energy budget. *Journal of Geophysical Research-Atmospheres*, 122, 3806– 3820. https://doi.org/10.1002/2016JD026278

Mcculley, R. L., Archer, S. R., Boutton, T. W., Hons, F. M., & Zuberer, D. A. (2004). Soil respiration and nutrient cycling in wooded communities developing in grassland. *Ecology*, 85, 2804– 2817. https://doi.org/10.1890/03-0645

Mcculley, R. L., & Jackson, R. B. (2012). Conversion of Tallgrass Prairie to Woodland: Consequences for Carbon and Nitrogen Cycling. *American Midland Naturalist*, 167, 307– 321. https://doi.org/10.1674/0003-0031-167.2.307

Mckinley, D. C., & Blair, J. M. (2008). Woody plant encroachment by *Juniperus virginiana* in a mesic native grassland promotes rapid carbon and nitrogen

accrual. *Ecosystems*, 11, 454– 468. https://doi.org/10.1007/s10021-008-9133-4

Mildrexler, D., Yang, Z. Q., Cohen, W. B., & Bell, D. M. (2016). A forest vulnerability index based on drought and high temperatures. *Remote Sensing of Environment*, 173, 314– 325. https://doi.org/10.1016/j.rse.2015.11.024

Msanne, J., Awada, T., Bryan, N. M., Schacht, W., Drijber, R., Li, Y., … Hiller, J. (2017). Ecophysiological responses of native invasive woody *Juniperus virginiana* L. to resource availability and stand characteristics in the semiarid grasslands of the Nebraska Sandhills. *Photosynthetica*, 55, 219– 230. https://doi.org/10.1007/s11099-016-0683-y

Mu, Q. Z., Zhao, M. S., & Running, S. W. (2011). Improvements to a MODIS global terrestrial evapotranspiration algorithm. *Remote Sensing of Environment*, 115, 1781– 1800. https://doi.org/10.1016/j.rse.2011.02.019

Mu, Q., Zhao, M., & Running, S. W. (2013). MODIS Global Terrestrial Evapotranspiration (ET) Product (NASA MOD16A2/A3). Algorithm Theoretical Basis Document, Collection 5. NASA Headquarters.

O'Donnell, F. C., & Caylor, K. K. (2012). A model-based evaluation of woody plant encroachment effects on coupled carbon and water cycles. *Journal of Geophysical Research-Biogeosciences*, 117, G02012.

Pacala, S. W., Hurtt, G. C., Baker, D., Peylin, P., Houghton, R. A., Birdsey, R. A., … Field, C. B. (2001). Consistent land- and atmosphere-based US carbon sink estimates. *Science*, 292, 2316– 2320. https://doi.org/10.1126/science.1057320

Paulo, A. A., Rosa, R. D., & Pereira, L. S. (2012). Climate trends and behaviour of drought indices based on precipitation and evapotranspiration in Portugal. *Natural Hazards and Earth System Sciences*, 12, 1481– 1491. https://doi.org/10.5194/nhess-12-1481-2012

Peel, M. C., Finlayson, B. L., & Mcmahon, T. A. (2007). Updated world map of the Koppen-Geiger climate classification. *Hydrology and Earth System Sciences*, 11, 1633– 1644. https://doi.org/10.5194/hess-11-1633-2007

Peng, S. S., Piao, S. L., Zeng, Z. Z., Ciais, P., Zhou, L., Li, L. Z. X., … Zeng, H. (2014). Afforestation in China cools local land surface temperature. *Proceedings of the National Academy of Sciences of the United States of America*, 111, 2915– 2919. https://doi.org/10.1073/pnas.1315126111

Petrie, M. D., Collins, S. L., Swann, A. M., Ford, P. L., & Litvak, M. E. (2015). Grassland to shrubland state transitions enhance carbon sequestration in the northern Chihuahuan Desert. *Global Change Biology*, 21, 1226– 1235. https://doi.org/10.1111/gcb.12743

Poulter, B., Frank, D., Ciais, P., Myneni, R. B., Andela, N., Bi, J., … van der Werf, G. R. (2014). Contribution of semi-arid ecosystems to interannual variability of the global carbon cycle. *Nature*, 509, 600– 603. https://doi.org/10.1038/nature13376

Qiao, L., Zou, C. B., Will, R. E., & Stebler, E. (2015). Calibration of SWAT model for woody plant encroachment using paired experimental watershed data. *Journal of Hydrology*, 523, 231– 239. https://doi.org/10.1016/j.jhydrol.2015.01.056

Qin, Y., Xiao, X., Wang, J., Dong, J., Ewing, K., Hoagland, B., … Loveland, T. (2016). Mapping annual forest cover in sub-humid and semi-arid regions through analysis of landsat and PALSAR imagery. *Remote Sensing*, 8, 933. https://doi.org/10.3390/rs8110933

Ratajczak, Z., Nippert, J. B., & Collins, S. L. (2012). Woody encroachment decreases diversity across North American grasslands and savannas. *Ecology*, 93, 697– 703. https://doi.org/10.1890/11-1199.1

Ratajczak, Z., Nippert, J. B., Hartman, J. C., & Ocheltree, T. W. (2011). Positive feedbacks amplify rates of woody encroachment in mesic tallgrass prairie. *Ecosphere*, 2, art121.

Running, S. W., Mu, Q., Zhao, M., & Moreno, A. (2017). MODIS Global Terrestrial Evapotranspiration (ET) Product (NASA MOD16A2/A3) NASA Earth Observing System MODIS Land Algorithm.

Schwalm, C. R., Williams, C. A., Schaefer, K., Arneth, A., Bonal, D., Buchmann, N., … Richardson, A. D. (2010). Assimilation exceeds respiration sensitivity to drought: A FLUXNET synthesis. *Global Change Biology*, 16, 657– 670. https://doi.org/10.1111/j.1365-2486.2009.01991.x

Scott, R. L., Biederman, J. A., Hamerlynck, E. P., & Barron-Gafford, G. A. (2015). The carbon balance pivot point of southwestern US semiarid ecosystems: Insights from the 21st century drought. *Journal of Geophysical Research-Biogeosciences*, 120, 2612– 2624. https://doi.org/10.1002/2015JG003181

Scott, R. L., Huxman, T. E., Barron-Gafford, G. A., Jenerette, G. D., Young, J. M., & Hamerlynck, E. P. (2014). When vegetation change alters ecosystem water availability. *Global Change Biology*, 20, 2198– 2210. https://doi.org/10.1111/gcb.12511

Scott, R. L., Huxman, T. E., Williams, D. G., & Goodrich, D. C. (2006). Ecohydrological impacts of woody-plant encroachment: Seasonal patterns of water and carbon dioxide exchange within a semiarid riparian environment. *Global Change Biology*, 12, 311– 324. https://doi.org/10.1111/j.1365-2486.2005.01093.x

Scott, R. L., Jenerette, G. D., Potts, D. L., & Huxman, T. E. (2009). Effects of seasonal drought on net carbon dioxide exchange from a woody-plant-

encroached semiarid grassland. *Journal of Geophysical Research-Biogeosciences*, 114, G04004.

Spera, S. A., Galford, G. L., Coe, M. T., Macedo, M. N., & Mustard, J. F. (2016). Land-use change affects water recycling in Brazil's last agricultural frontier. *Global Change Biology*, 22, 3405– 3413. https://doi.org/10.1111/gcb.13298

Tucker, C. J. (1979). Red and photographic infrared linear combinations for monitoring vegetation. *Remote Sensing of Environment*, 8, 127– 150. https://doi.org/10.1016/0034-4257(79)90013-0

Van Els, P., Will, R. E., Palmer, M. W., & Hickman, K. R. (2010). Changes in forest understory associated with *Juniperus* encroachment in Oklahoma, USA. *Applied Vegetation Science*, 13, 356– 368.

Velpuri, N. M., Senay, G. B., Singh, R. K., Bohms, S., & Verdin, J. P. (2013). A comprehensive evaluation of two MODIS evapotranspiration products over the conterminous United States: Using point and gridded FLUXNET and water balance ET. *Remote Sensing of Environment*, 139, 35– 49. https://doi.org/10.1016/j.rse.2013.07.013

Vicente-Serrano, S. M., Begueria, S., & Lopez-Moreno, J. I. (2010). A multiscalar drought index sensitive to global warming: The Standardized Precipitation Evapotranspiration Index. *Journal of Climate*, 23, 1696– 1718. https://doi.org/10.1175/2009JCLI2909.1

Vicente-Serrano, S. M., Begueria, S., Lorenzo-Lacruz, J., Camarero, J. J., López-Moreno, J. I., Azorin-Molina, C., … Sanchez-Lorenzo, S. (2012). Performance of drought indices for ecological, agricultural, and hydrological applications. *Earth Interactions*, 16, 1– 27. https://doi.org/10.1175/2012EI000434.1

Wagle, P., Xiao, X., Torn, M. S., Cook, D. R., Matamala, R., Fischer, M. L., … Biradar, C. (2014). Sensitivity of vegetation indices and gross primary production of tallgrass prairie to severe drought. *Remote Sensing of Environment*, 152, 1– 14. https://doi.org/10.1016/j.rse.2014.05.010

Wang, J., Xiao, X., Qin, Y., Dong, J., Geissler, G., Zhang, G., … Doughty, R. B. (2017). Mapping the dynamics of eastern redcedar encroachment into grasslands during 1984–2010 through PALSAR and time series Landsat images. *Remote Sensing of Environment*, 190, 233– 246. https://doi.org/10.1016/j.rse.2016.12.025

Wang, J., Xiao, X., Qin, Y., Doughty, R. B., Dong, J., & Zou, Z. (2018). Characterizing the encroachment of juniper forests into sub-humid and semi-arid prairies from 1984 to 2010 using PALSAR and Landsat data. *Remote Sensing of Environment*, 205, 166– 179.

Wang, J., Xiao, X. M., Wagle, P., Ma, S., Baldocchi, D., Carrara, A., … Qin, Y. (2016). Canopy and climate controls of gross primary production of Mediterranean-type deciduous and evergreen oak savannas. *Agricultural and*

Forest Meteorology, 226, 132– 147. https://doi.org/10.1016/j.agrformet.2016.05.020

Willson, C. J., Manos, P. S., & Jackson, R. B. (2008). Hydraulic traits are influenced by phylogenetic history in the drought-resistant, invasive genus *Juniperus* (Cupressaceae). *American Journal of Botany*, 95, 299– 314. https://doi.org/10.3732/ajb.95.3.299

Wine, M. L., & Hendrickx, J. M. H. (2013). Biohydrologic effects of eastern redcedar encroachment into grassland, Oklahoma, USA. *Biologia*, 68, 1132– 1135.

Xiao, X. M., Hollinger, D., Aber, J., Goltz, M., Davidson, E. A., Zhang, Q. Y., & Moore, B. (2004). Satellite-based modeling of gross primary production in an evergreen needleleaf forest. *Remote Sensing of Environment*, 89, 519– 534. https://doi.org/10.1016/j.rse.2003.11.008

Yang, X., Tang, J. W., Mustard, J. F., Lee, J.-E., Rossini, M., Joiner, J., … Richardson, A. D. (2015). Solar-induced chlorophyll fluorescence that correlates with canopy photosynthesis on diurnal and seasonal scales in a temperate deciduous forest. *Geophysical Research Letters*, 42, 2977– 2987. https://doi.org/10.1002/2015GL063201

Yu, M. X., Li, Q. F., Hayes, M. J., Svoboda, M. D., & Heim, R. R. (2014). Are droughts becoming more frequent or severe in China based on the Standardized Precipitation Evapotranspiration Index: 1951–2010? *International Journal of Climatology*, 34, 545– 558. https://doi.org/10.1002/joc.3701

Zhang, Y., Xiao, X. M., Jin, C., Dong, J., Zhou, S., Wagle, P., … Moore III, B. (2016). Consistency between sun-induced chlorophyll fluorescence and gross primary production of vegetation in North America. *Remote Sensing of Environment*, 183, 154– 169. https://doi.org/10.1016/j.rse.2016.05.015

Zhang, Y., Xiao, X. M., Wu, X. C., Zhou, S., Zhang, G. L., Qin, Y. W., & Dong, J. W. (2017). Data descriptor: A global moderate resolution dataset of gross primary production of vegetation for 2000-2016. *Scientific Data*, 4, 170165. https://doi.org/10.1038/sdata.2017.165

Zhang, Y., Xiao, X., Zhang, Y., Wolf, S., Zhou, S., Joiner, J., … de Grandcourt, A. (2018). On the relationship between sub-daily instantaneous and daily total gross primary production: Implications for interpreting satellite-based SIF retrievals. *Remote Sensing of Environment*, 205, 276– 289. https://doi.org/10.1016/j.rse.2017.12.009

Zhou, Y. T., Xiao, X. M., Wagle, P., Bajgain, R., Mahan, H., Basaram, J. B., … Steiner, J. L. (2017). Examining the short-term impacts of diverse management practices on plant phenology and carbon fluxes of Old World bluestems pasture. *Agricultural and Forest Meteorology*, 237, 60– 70. https://doi.org/10.1016/j.agrformet.2017.01.018

Zou, C. B., Qiao, L., & Wilcox, B. P. (2016). Woodland expansion in central Oklahoma will significantly reduce streamflows – A modelling analysis. *Ecohydrology*, 9, 807– 816. https://doi.org/10.1002/eco.1684

Zou, C. B., Turton, D. J., Will, R. E., Engle, D. M., & Fuhlendorf, S. D. (2014). Alteration of hydrological processes and streamflow with juniper (*Juniperus virginiana*) encroachment in a mesic grassland catchment. *Hydrological Processes*, 28, 6173– 6182. https://doi.org/10.1002/hyp.10102